17th Australasian Fluid Mechanics Conference
Auckland, New Zealand
5-9 December 2010

Fuel Injection via Rectangular Cross-section Injectors for Mixing Enhancement in Scramjets

V. Wheatley[1] and P.A. Jacobs[1]

[1]School of Mechanical and Mining Engineering
University of Queensland, Queensland 4072, Australia

Abstract

We investigate the mixing enhancement provided by rectangular injectors in a flow applicable to inlet injection in scramjets: oblique injection into a cross-flow with a high supersonic Mach number. This is accomplished via three-dimensional Reynolds-averaged Navier-Stokes simulations. The near field mixing efficiency is quantified for all cases investigated and is seen to be closely linked to the generation of streamwise vorticity in the jet-cross-flow interaction. The production of streamwise voritcity is quantified and its impact on the flow physics is discussed.

Introduction

Injecting fuel in a scramjet inlet is a technique that allows the fuel to have more time to mix with the inflowing air, subsequently enabling it to be combusted efficiently [1]. Fuel is typically injected through circular port holes at an oblique angle to the flow. Oblique fuel injection contributes to the specific thrust of the scramjet [2]. Although inlet injection has been successful for the Mach numbers investigated previously, at flight Mach numbers greater than ten, the residence time in the engine becomes shorter, thus the mixing performance is more critical. Billig [2] identified mixing enhancement at high Mach numbers as one of the key technical issues that must be overcome to realize the full potential of the scramjet.

Diamond shaped injectors have been extensively investigated as an alternative to circular port holes. Tomioka, *et al*. [3] found that they generally resulted in greater jet penetration than equivalent area circular injectors. In a recent study, Foster and Engblom [4] found that for normal injection into a Mach 1.2 cross-flow, rectangular injectors that are longer in the stream-wise direction produce significantly increased mixing over circular or diamond shaped injectors. They postulate this is due to an increased production of streamwise vorticity in the jet-cross-flow interaction. Mack *et al*. [5,6] have investigated the performance of rectangular cross-section (slot) injectors for scramjet combustor conditions and similarly report an increase in mixing efficiency. However, they simultaneously investigate mixing enhancement due to shock impingement on the fuel jet, making it difficult to determine the benefit of the non-circular injectors. In the surveyed literature, the mechanism underlying the enhanced mixing produced by slot injectors is not presented in detail. The focus of our investigation is to address this.

We investigate the mixing enhancement provided by rectangular injectors in a case applicable to inlet injection in scramjets: oblique injection into a cross-flow with a high supersonic Mach number. This paper is structured as follows: first, we define the problem geometry and flow conditions under consideration and provide details of our computational approach. We then define measures of injector performance, including a measure of their streamwise vorticity production. To allow an incremental approach to describing the mixing enhancement mechanisms, we next present results for the inviscid case. The results of viscous, turbulent simulations are analysed following this. Finally the conclusions that have been drawn from this investigation are presented.

Modelling Approach

The geometry of the problem under consideration is shown in figure 1. A sonic jet of hydrogen is injected into a supersonic cross-flow of air through an l by w slot at an angle of 45° to the freestream. The stagnation temperature and pressure of the hydrogen were selected to be 300 K and 1 MPa, respectively. The cross-flow of air is at Mach 5 with a temperature of 770.0 K and a pressure of 13.68 kPa. This corresponds to conditions following the primary stages of compression for a scramjet with flight Mach number M_∞ = 10 at an altitude of 25.75 km, where p_∞ = 2219.3 Pa and T_∞ = 219.9 K. Both gases are taken to be a calorically perfect with γ = 1.4. To reduce computational expense, a symmetry plane is applied through the jet centerline allowing only half the flow to be simulated.

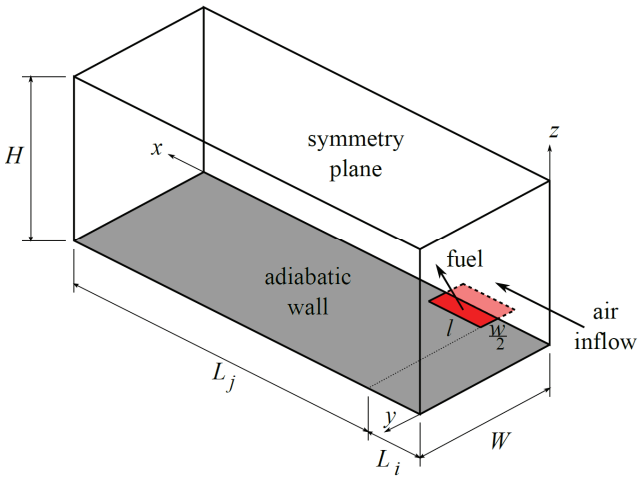

Figure 1. Simulation geometry including coordinate system

The baseline jet cross-section is a $d \times d$ = 1 mm^2 square (corresponds to $l = 2^{1/2}d$, $w=d$). For the simulated jet length $L_j = 32d$, the height and width of the domain were selected to be H = $16d$ and W = $12d$ so that the shocks generated by the interaction did not reflect from the domain boundaries and impinge on the jet. This allows us to study the mixing enhancement due to varying the injector cross-section in isolation from that due to shock impingement. The computational domain extends a distance L_i upstream of the fuel jet to capture the upstream separated flow and the bow shock. For viscous simulations L_i is set to $10d$ and for inviscid simulations $4d$ is more than sufficient.

Simulations were carried out in three dimensions using the compressible Navier-Stokes solver Eilmer3 [7]. This solver is second-order accurate and utilizes the EFM flux solver near shocks and the AUSMDV flux elsewhere. The simulations

utilized a k-ω turbulence model with the free-steam (inflow) turbulence intensity and turbulent viscosity ratio taken to be 0.05 and 0.1, respectively. The turbulent Prandtl number was set to 0.89 and the turbulent Schmidt number was set to 0.75. Note that as we do not model the scalar variance, we effectively study macroscopic stirring rather than microscopic mixing. The lower wall aside from the fuel injection slot is taken to be an adiabatic, no-slip wall. A zero gradient boundary condition is applied on outflow boundary at the end of the domain. Fixed inflow conditions applied at the fuel and air inlets. All other boundaries are symmetry planes.

For viscous simulations, the computational domain is discretised into 290 cells in the x-direction, 82 cells in the y-direction and 100 cells in the z-direction. To adequately capture the boundary layer, fuel inlet and mixing layers, the grid is heavily clustered towards the wall and fuel injection locations. This results in the maximum z^+ value of cells along the no-slip wall being less than 1.8 (≈0.2 in the undisturbed boundary layer), with similar resolution in the mixing layers. The simulations were run as unsteady Reynolds-averaged Navier-Stokes (URANS) simulations for 0.04 ms, by which time the mean flow becomes steady. The insensitivity of relevant statistics to the grid was established by repeating the simulation of the baseline case with 0.5 and 1.25 times the resolution in each direction. In order to inject the fuel through a realistic thickness boundary layer without simulating its full development, the inflow condition includes a turbulent boundary layer profile adjacent to the bottom wall. The profile was computed using the same solver and corresponds to a tripped, zero pressure gradient boundary layer 0.1 m from its origin. The thickness of the boundary layer 10d upstream of the fuel jet is approximately 4d.

For inviscid simulations, 200, 70 and 60 cells were used in the x-, y- and z-directions, respectively. As there is no physical viscosity to set a minimum length-scale in inviscid simulations, solutions will continue to vary as the grid is refined and the numerical viscosity is decreased. Inviscid simulations were also run for 0.04 ms.

Injector Performance Measures

A number of parameters are required to adequately assess the performance of a scramjet fuel injector. To assess the ability of the injector to rapidly mix fuel (H_2) and air, we use the following mixing efficiency base on the fuel stream,

$$\eta_m(x) = \frac{1}{\dot{m}_{H_2}} \int_x \min\left(f_{H_2}, \frac{f^s_{H_2}}{f^s_{O_2}} f_{O_2}\right) d\dot{m},$$

where $f^s_{H_2}$ = 0.02876 and $f^s_{O_2}$ = 0.22824 are the stoichiometric mass fractions of hydrogen and oxygen, respectively, and $\dot{m}_{H_2}$ is the total mass flow rate of hydrogen. This indicates the fraction of fuel that would be consumed if all mixed fuel and air reacted.

Many devices that enhance mixing, such as hypermixers, can also lead to a greater loss in stagnation pressure (p_0) which reduces thrust. Stagnation pressure losses are due to shocks, viscous forces and mixing and may be characterised [5] by,

$$\Pi(x) = 1 - \frac{\int_x \rho u p_0 dA}{\int_{x=0} \rho u p_0 dA},$$

Where ρ is the density, u is the streamwise velocity and x = 0 is the inflow plane of our domain.

Another important metric for a wall injector is the jet penetration, as this influences how quickly fuel can mix with the airflow near the centreline of the engine. Jet penetration is often defined as the visible height of the jet from the wall. In the spirit of this definition, we take the jet penetration P to be the maximum height for which $f_{H_2} > 0.1\, f^s_{H_2}$ in a give, cross-section.

Finally, we need to characterise the streamwise vorticity, ω_x, produced by the jet-cross-flow interaction. Vortices enhance mixing by stretching and wrapping up the interfaces between fluids, greatly increasing the interfacial area across which molecular diffusion can act. As both signs of vorticity can lead to enhanced mixing, we simply utilise the integral of the absolute value of the streamwise vorticity,

$$\Gamma(x) = \frac{1}{UD} \int_x |\omega_x| \mathrm{dA},$$

where U is the freestream velocity of the crow-flow and D is the effective diameter of the injector.

Inviscid Results

Inviscid simulations were carried out for jet aspect ratios (l:w) of 1:4, 1:1, 4:1 and 16:1, with the area of the cross-section maintained at d^2 for all cases. The resulting distributions of mixing efficiency are shown in figure 2(a). The mixing efficiency downstream of the injector increases uniformly with aspect ratio. This is highly correlated with the peak streamwise circulation, which is shown in figure 2(b). While the rate of streamwise vorticity production is lower for higher aspect ratio cases, production is maintained over a greater streamwise length, resulting in a higher peak circulation.

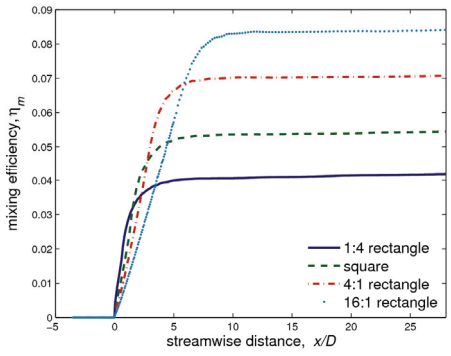

(a)

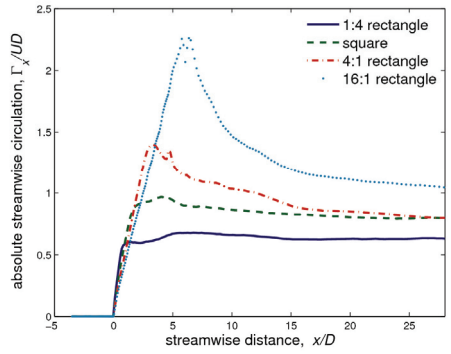

(b)

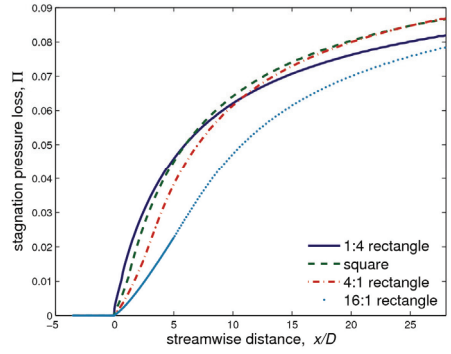

(c)

Figure 2. Profiles of (a) mixing efficiency, (b) absolute streamwise circulation and (c) stagnation pressure loss for inviscid simulations.

Fuel injected near the upstream edge of the injector slot creates a partial blockage of the cross-stream, allowing the fuel injected further downstream to penetrate further. This allows a high aspect ratio streamwise slot injector to generate a strong, high curvature bow shock that persists over a greater length and height than a lower aspect ratio injector. This can be seen in figure 3, which shows the bow shock shapes generated by 1:4 and 16:1 aspect ratio injectors. Figure 2(c) shows the stagnation pressure losses for the inviscid cases. The highest aspect ratio injector exhibits the lowest loss, despite its more persistent strong bow shock and higher mixing. This is due to the near-normal portion of the shocks (including the fuel barrel shock) adjacent to the injector leading edge, which produce the highest losses, being of much lower area than for the other cases. Note that the variation of stagnation pressure loss with aspect ratio is non-monotonic due to the competing effects mentioned above.

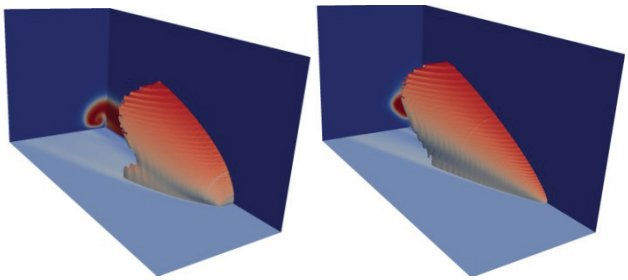

Figure 3. Isosurfaces of pressure near injectors showing bow shocks generated by (left) 1:4 and (right) 16:1 slot injectors. Isosurfaces appear where the shocks have a pressure ratio greater than 30. Isosurfaces coloured by the z-component of its normal vector. Bottom walls show temperature contours, others show fuel mass fraction contours.

We now turn our attention to the cause of the increased streamwise vorticity production for the high aspect ratio injectors. The jet studied here is highly underexpanded, thus the fuel rapidly expands as it leaves the injector and is subsequently compressed by the barrel shock. Following these processes, the fuel along the sides of the jet retains a significantly different velocity to the neighbouring air. This results in shear layers forming adjacent to the barrel shock. The shear layers emanating from the spanwise sides of the injector have a significant component of their vorticity in the streamwise direction, as can be seen in figure 6. This vorticity is convected upwards, outwards and downstream by the combined action of the jet and crossflow, forming a pair of counter-rotating wake vortices. The amount of streamwise vorticity generated in this manner is directly related to the streamwise length of the injector, resulting in the increased production seen for high aspect ratio injectors, which in turn enhances mixing. The second peak in vorticity that can be seen in high aspect ratio profiles in figure 2(b) is due to the formation of another pair of counter-rotating wake vortices. This pair of vortices is observed to form near the symmetry plane adjacent to the termination of the barrel shock. These subsequently merge with the pair of vortices described above, resulting in the vortex pairs shown in figure 4 for each inviscid case. For high aspect ratios, we observe that the stronger induced flow of the wake vortices results in the formation of a pair of vortices with the opposite sign of rotation at the corners between the wall and the symmetry plane.

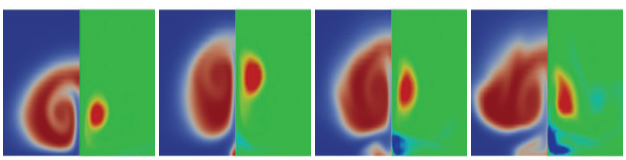

Figure 4. Spanwise cross-sections of near-jet flow at x/d = 35 for (from left to right) 1:4, 1:1, 4:1 and 16:1 aspect ratio fuel jets. The left half of each plot shows fuel mass fraction contours, the right half shows mirrored streamwise vorticity contours. Each frame uses the same contour levels.

Viscous Results

To determine how the presence of viscous effects and a relatively thick turbulent boundary layer affects the picture of mixing enhancement developed from the inviscid simulations, we have carried out dissipative, turbulent simulations of the square and 16:1 aspect ratio fuel jets. The resulting mixing efficiencies are compared to the inviscid cases in figure 5(a). The main effect observed is that mixing continues at a much higher rate downstream of the injector in the viscous cases. This is in part due to the enhanced transport due to diffusion and turbulence, but we will demonstrate that other mechanisms also contribute. Figure 5(b) compares the streamwise circulation profiles. The circulation is much higher in the viscous cases, but figure 5(a) shows that this does not result in an increase in mixing of the same magnitude. This is partially accounted for by the spanwise deflection of the airflow causing the vorticity in the boundary layer to have a streamwise component, which does not contribute directly to the mixing. The jet penetration for the cases under consideration is shown in figure 5(c). Unlike in the inviscid case, the streamwise slot injector produces lower jet penetration than the square injector in the viscous case.

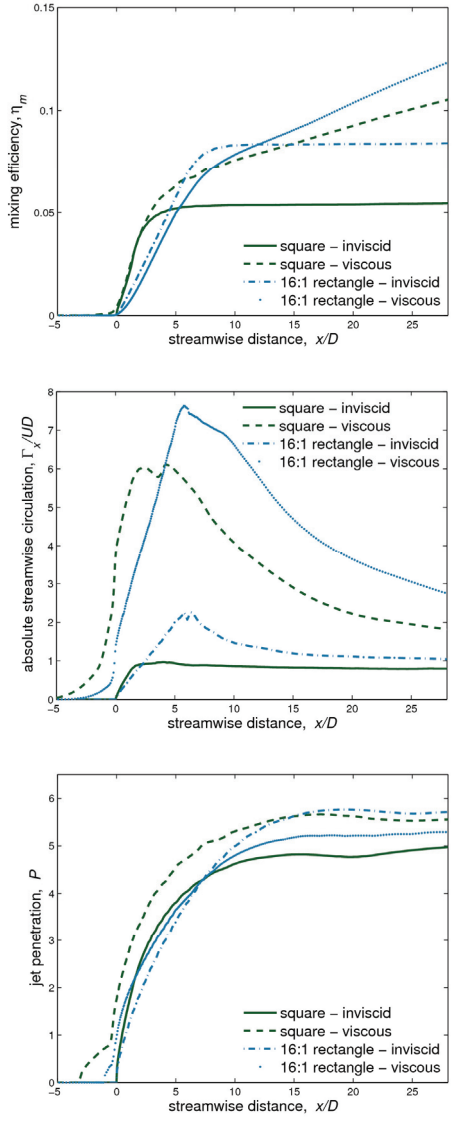

Figure 5. Profiles of (a) mixing efficiency, (b) absolute streamwise circulation and (c) jet penetration for inviscid and turbulent simulations of the square and 16:1 aspect ratio jets.

In addition to increased transport, mixing is enhanced in the viscous case due to the formation of additional vortex pairs, as can be seen in figure 6, which shows cross-sections of the 16:1 fuel jets 6*d* from the beginning of injection. Of particular significance for mixing is the wake vortex pair forming adjacent to the barrel shock shear layer. We believe this corresponds to "trailing vortex 2" identified by Viti *et al.* [8]. This vortex originates from the shear layer between the leading edge of the fuel jet and the separated flow upstream of it. It is then convected downstream and upwards along the barrel shock [8]. As it is convected, we assert that it grows by entraining fluid and hence vorticity from the shear layer adjacent to the barrel shock, as indicated by figure 6.

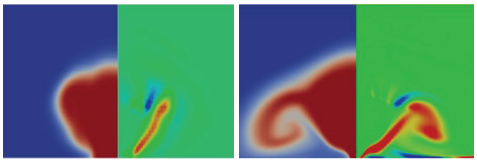

Figure 6. Inviscid (left) and viscous (right) spanwise cross-sections of near-jet flow 6*d* from the beginning of injection for the 16:1 aspect ratio fuel jet. The left half of each plot shows fuel mass fraction, the right half shows mirrored streamwise vorticity. Frames use equal contour levels.

Figure 7 shows jet cross-sections for the square and 16:1 viscous cases at various streamwise locations. The vortex pair discussed above is also present in the square jet case. However, it is comparatively weak and rapidly merges with the wake vortices identified in the inviscid case. The explanation for this is that it has a shorter length of shear layer from which to entrain vorticity. In both cases, the inward flow induced by the vortices generates vorticity of the opposite sign at the wall, which is subsequently swept upwards at the centreline, further enhancing the mixing.

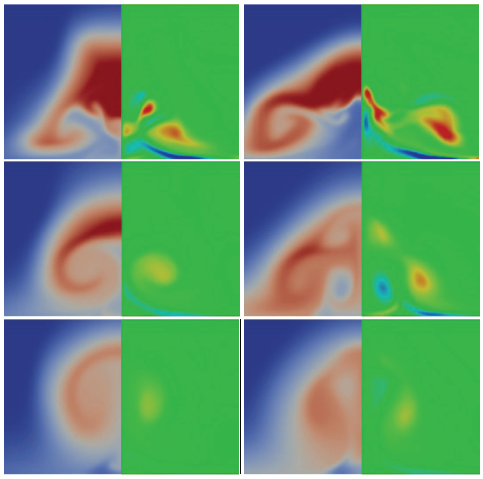

Figure 7. Spanwise cross-sections of near-jet flow 8*d* (top), 18*d* (middle) and 32*d* (bottom) from the beginning of injection for the square (left) and 16:1 (right) aspect ratio fuel jet. The left half of each plot shows fuel mass fraction contours, the right half shows mirrored streamwise vorticity contours. Each frame uses the same contour levels.

Sample streamlines for the viscous cases are shown in figure 8. The streamlines originating in air near the wall demonstrate the presence of the horse-shoe vortex, which is stronger in the square jet case. The horse-shoe vortex originates for the separated flow upstream of the injector. The effect of the additional vortices discussed is clearly seen in the streamlines originating from the fuel jet in figure 8(b). The streamlines originating closest to the edge of the jet are initially swept outwards, then downwards and inwards close to the wall. They are then swept upwards through the centreline of the jet and terminate on the upper surface of the jet. Some streamlines originating slightly further from the boundary are swept outwards and never re-enter the jet core, producing the well mixed fluid seen between the jet core and the horse-shoe vortex. Finally, streamlines originating near the centreline of the injector follow trajectories that appear to the chiefly governed by the wake vortices seen in the inviscid case.

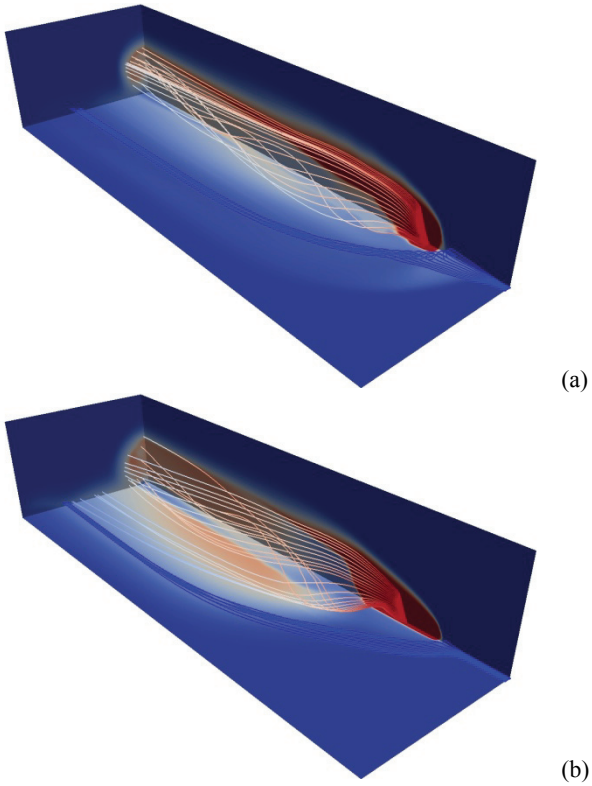

Figure 8. Streamlines colored by fuel mass fraction for the viscous (a) square and (b) 16:1 aspect ratio jets. Planes show fuel mass fraction.

Conclusions

We find that in both inviscid and dissipative, turbulent simulations, high aspect ratio streamwise slot injectors produce higher near field mixing efficiencies than lower aspect ratio jets, while causing a lower stagnation pressure loss. The mixing enhancement is driven by the increased streamwise vorticity production at the spanwise edges of the jet interaction.

References

[1] Stalker, R.J., Paull, A., Mee, D.J., Morgan R.G., & Jacobs, P.A., Scramjets and shock tunnels - The Queensland experience, *Progress in Aerospace Sciences*, **41**, 2005, 471-513.

[2] Billig, F.S., Research on supersonic combustion, *42nd Aerospace Sciences Meeting and Exhibit*, Reno, Nevada, 1995, AIAA-92-0001.

[3] Tomioka, S., Jacobsen, L.S. & Schetz, J.A., Sonic Injection from Diamond-Shaped Orifices into a Supersonic Crossflow, *J. of Propulsion and Power*, **19**, 2003, 104-114.

[4] Foster, L.E. & Engblom, W.A., Computation of Transverse Injection Into Supersonic Crossflow With Various Injector Orifice Geometries, in *42nd Aerospace Sciences Meeting and Exhibit*, Reno, Nevada, January 5–8, 2004, AIAA–2004–1199.

[5] Mack, A. & Steelant, J., Mixing enhancement by shock impingement in a generic scramjet combustion chamber, in *European Conference on Computational Fluid Dynamics*, Noordwijk, The Netherlands, 2006.

[6] Mack, A., Steelant, J., Hannemann, K., Karl, S. & Odam, J., Mixing and combustion enhancement in a generic scramjet combustion chamber, in *14th AIAA/AHI Space Plance and Hypersonic Systems and Technologies Conference*, 2006, AIAA 2006-8134.

[7] Jacobs, P.A. & Gollan, R.J., *The Elmer3 Code: User Guide and Example Book*, The University of Queensland Mechanical Engineering Report 2008/07, 2008.

[8] Viti, V., Neel, R. & Schetz, J.A., Detailed flow physics of the supersonic jet interaction flow field, *Phys. Fluids*, **21**, 2009, 046101.